Applied Physics B (2019) 125:181
https://doi.org/10.1007/s00340-019-7294-9

Applied Physics B
Lasers and Optics

Particle size and concentration effect on thermal diffusivity of water-based ZnO nanofluid using the dual-beam thermal lens technique

M. Ramya[1] · T. K. Nideep[1] · V. P. N. Nampoori[1] · M. Kailasnath[1]

Received: 4 June 2019 / Accepted: 23 August 2019 / Published online: 31 August 2019

Abstract
In the present work, we experimentally investigate the size and concentration dependence of the thermal diffusivity of water-based ZnO nanofluid. The results show an increase in thermal diffusivity both by increasing the particle size from 5.6 to 16.6 nm as well as nanoparticle concentration in the range 0.02–0.1 mg/ml. It was also observed that there is a 4% enhancement in thermal diffusivity of the nanofluid for an optimum value of nanoparticle size and concentration. The dependence of thermal diffusivity on the particle size and concentration can give a great insight into the inter-particle interaction and the aggregation dynamics in nanofluid.

1 Introduction

Nanofluids are termed as a new class of heat transfer fluids that exhibits important thermophysical properties. It is well known that the nanoparticles of the order of 1–100 nm when suspended into the base fluids can enhance the heat transfer mechanism [1–12]. Nanofluids can be considered as next-generation heat transfer fluids, which have the potential to reduce the thermal resistance compared to conventional fluids as well as fluids containing micro-sized particles. Conventional liquids such as water, ethylene glycol, decene, silicon oil, and engine oil are normally used as heat transfer liquids. When micro-sized particles are suspended in such fluids, there is a chance that they settle down due to higher size and density. Since the above process introduces an additional flow resistance and erosion, micro-fluids have not yet been commercialized [4, 10, 12, 13].

Nanoparticles possess larger surface area compared to conventional particles thereby significantly improving the stability and heat transfer capacity. Nanofluids are finding applications in numerous fields such as microelectronics, microfluidics, medical, instrumentation, transportation, MEMS and HVAC systems [2, 5, 6, 12, 14]. Several possible mechanisms such as Brownian motion, fluid convection, liquid layering at the particle–fluid interface and cluster agglomeration can affect the heat transfer enhancement in nanofluids [1, 6, 15].

Nanofluid is not a simple mixture of nanoparticles and base fluid. To prepare effective nanofluids, proper dispersion and stabilization of nanoparticles in the base fluid are essential. Homogenously dispersed nanofluids can be prepared using various techniques such as by (1) controlling the pH value of suspensions, (2) adding surfactants and (3) using ultrasonication. All the above techniques help to obtain stable suspensions by changing the surface properties of dispersed nanoparticles [2, 6, 7, 13, 16]. Two techniques are most commonly used for synthesizing the nanofluids: a two-step technique and a one-step technique. In the two-step method, nanoparticles are synthesized using a physical or chemical route and the prepared powder form of nanoparticles is dispersed in the base fluid. The one-step method simultaneously synthesizes and disperses the nanoparticles into a base fluid [2, 7, 8, 16–19].

Ceramics, metals, semiconductors, carbon nanotubes and composite materials are used for nanofluid preparation [2]. Several parameters such as nanoparticle volume concentration, particle materials, size and morphology of materials, base fluid materials, temperature, and surfactants can affect the heat transfer characteristics of a nanofluid [5, 6, 8, 20, 21]. Thermal conductivity is the ability of the materials to transfer or conduct the heat, which is an important parameter responsible for heat

✉ M. Kailasnath
kailas@cusat.ac.in

[1] International School of Photonics, Cochin University of Science and Technology, Kochi, India

transfer enhancement. Several theoretical models (Maxwell model, Hamilton–Crosser model, Yue–Choi model, Xue model, and Strauss–Pober model) have been proposed to explain the thermal conductivity in nanofluids [2, 8, 13, 22, 23]. In many existing models of thermal conductivity, experimental values are found to be deviated from theoretical values. To minimize these discrepancies to an extent, researchers measure other parameters such as viscosity and diffusivity. Thermal conductivity and dynamic viscosity depend on the above-mentioned parameters that affect the heat transfer mechanism [24, 25]. There is no general correlation between thermal conductivity and dynamic viscosity established due to the lack of a common understanding mechanism of nanofluids.

Thermal conductivity (k) of nanofluid is directly related to its thermal diffusivity (α) by $\alpha = \frac{k}{\rho C_p}$ where ρ is the fluid density and C_p is the specific heat capacity. Hence, the measurement of thermal diffusivity helps to determine the thermal conductivity. Thermal diffusivity is a material-specific property, which describes how quickly the material reacts to the change in their thermal environment. Material with large thermal diffusivity will react quickly to change in temperature than smaller thermal diffusivity materials that take longer time to reach a new equilibrium condition. In most of the photonic applications, high thermal diffusivity materials are required to dissipate the laser-induced heating [26].

Several techniques such as transient techniques, steady-state techniques and thermal comparator have been adopted for measuring thermal conductivity of nanofluids [20, 27–33]. In comparison with the above methods, thermal lens techniques have many advantages. This is a very sensitive, accurate and less time-consuming technique which can be carried out at room temperature. Additional advantage of thermal lens technique includes the determination of dn/dt, which contains information about polarizability, refractive index, thermal expansion coefficient, viscosity, etc. [34–42]. In this technique, the nanofluid is irradiated with a laser source of appropriate frequency and a transient thermal lens signal is produced within the nanofluid. By monitoring these signals, we can estimate the thermal diffusivity of nanofluid.

Zinc oxide (ZnO) is a wonderful semiconducting material with a wide range of unique properties and is used in numerous multidisciplinary fields [43–46]. In this paper, we discuss the synthesis of stable water-based ZnO nanofluids and its thermal diffusivity measurement using thermal lens technique. To the best of our knowledge, this is the first report on thermal lensing studies of ZnO nanoparticles dispersed in water. The thermal diffusivity of nanocolloids mainly depends on size, concentration and shape of the suspended particles. Optimization of these parameters is important to understand the heat conducting mechanism in the nanofluid. Hence, the effect of particle size and nanoparticle concentration in the solution on the thermal diffusivity has been discussed.

2 Experimental

2.1 Synthesis of ZnO nanoparticles

Size-varied ZnO nanoparticles were synthesized using solution method incorporating ultrasound sonication at various temperatures. Detailed description of the synthesis method and characterization such as XRD, absorption, and TEM has been described in the previously published work [47]. Particle size of the synthesized ZnO nanoparticles is 5.6 ± 0.61 nm, 7.5 ± 1.7 nm, 12.5 ± 1.4 nm and 16.6 ± 2.2 nm corresponding to the samples A, B, C and D [47]. Figure 1 shows the TEM images of synthesized ZnO nanoparticles.

2.2 Preparation of ZnO nanofluids

In the present work, nanofluids were prepared by a two-step method. The powder form of ZnO nanoparticles of sizes ranging from 5.6 to 16.6 nm in different volume fraction (0.02–0.1 mg/ml) was dispersed in water. To achieve good dispersion stability of ZnO nanoparticles in the water, ultrasonication (EQUITRON, SR.NO. 8442.030.53H.ACD:002) was employed with a frequency of 53 kHz and 100% of power factor for a period of 1 h at room temperature. Intensive ultrasonication intensively disperses the particles, reduces agglomeration and suppresses the tendency to form particle clusters. This method also helps to attain good stability for water-based ZnO nanofluids. Figure 2 shows the flow chart for the preparation of ZnO nanofluids.

2.3 Theoretical background of thermal lens technique

The thermal lens (TL) technique is a well-known laser photothermal spectroscopy. Photothermal spectroscopy is a non-destructive technique where the information is deduced by the direct detection of change in the thermo-optical properties due to the absorption of radiation by the sample [40, 48–50]. Photothermal techniques have two versions: (1) photothermal modulation spectroscopy (CW laser used for excitation) and (2) pulsed photothermal spectroscopy (pulsed laser used for excitation). In both cases, thermal waves are generated in the sample. Analysing time-dependent variation of the light intensity can gain information about thermo-optical properties of the medium, such as temperature coefficient of refractive index and the thermal diffusivity.

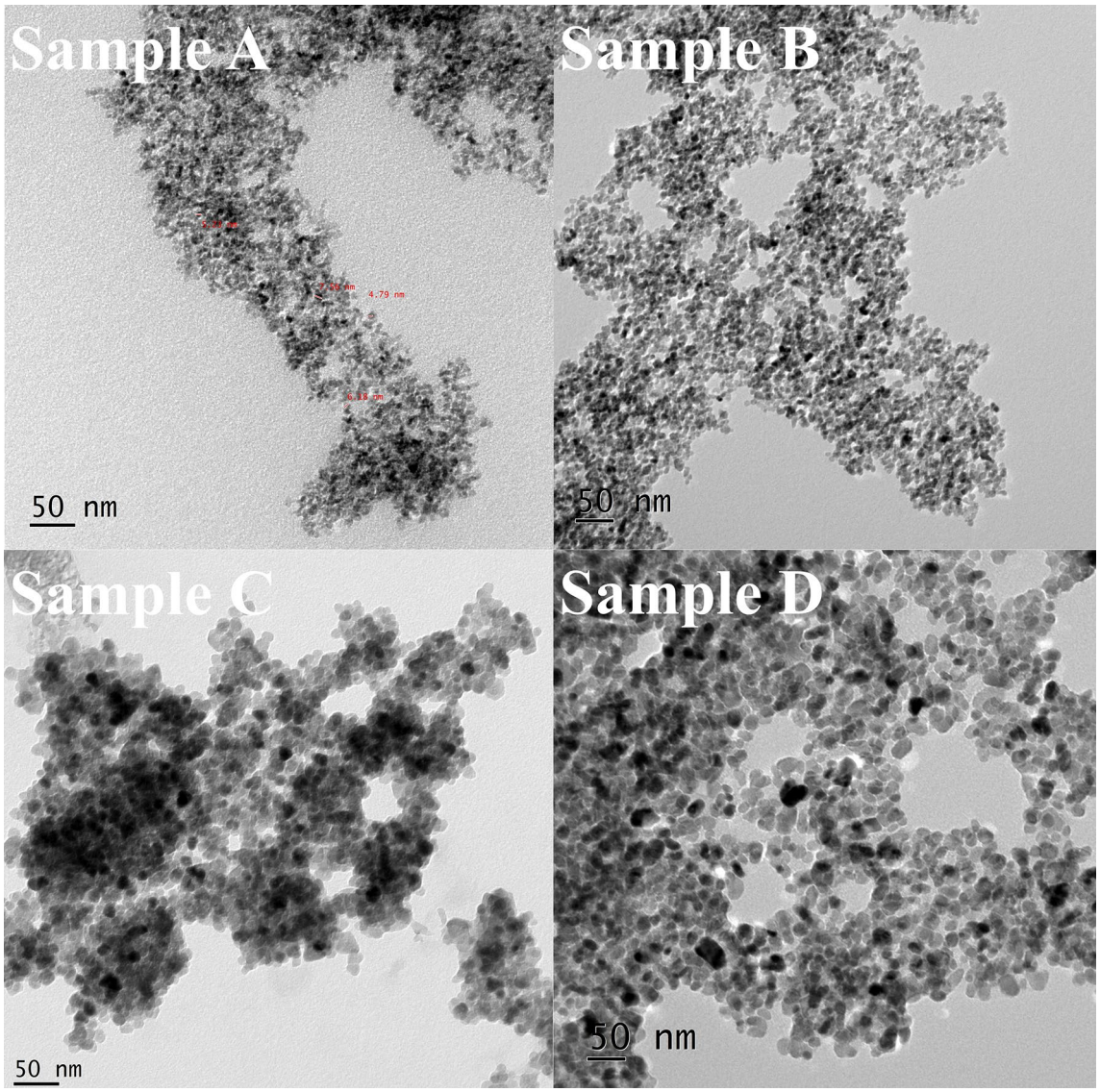

Fig. 1 TEM image of ZnO nanoparticles [47]

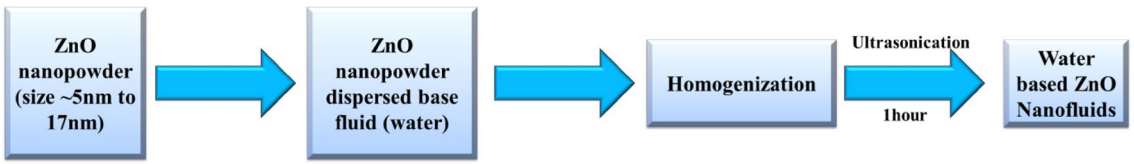

Fig. 2 Flow diagram of ZnO nanofluid preparation processes

In TL, the sample is irradiated by a laser beam of Gaussian intensity distribution (TEM_{00}) that generates a temperature gradient due to nonuniform heating [40, 48]. Consequently, refractive index (n) of the medium is changed producing a lensing effect. In more general cases, the variation of refractive index is given by

$$\Delta n = \left(\frac{\partial n}{\partial T}\right)_{\mathrm{P}} \Delta T + \left(\frac{\partial n}{\partial \rho}\right)_{\mathrm{T}} \Delta \rho.$$

The thermal lensing effect is observable for a laser in milliwatt or microwatt range provided the sample is transparent [40]. This effect can be generated using different pump or

probe beam geometries. In 1965, Gordon et al. [38] used a single-beam geometry where generation and probing thermal lens signals were achieved using a single laser beam. Optical simplicity and ease of optical alignment are the main advantages of single-beam arrangement. The dual-beam optical configuration utilizes two laser beams. One beam that is used to excite the sample forms the thermal lens. A second laser beam probes the lens created in the sample. Usually a high-power CW/pulsed laser is used as the pump beam, while the probe beam is a relatively weaker CW laser [48].

The dual-beam thermal lens instrumentation can be arranged in two configurations, longitudinal (collinear) and transverse. In most of the cases, a collinear configuration is used. Mode-matched and mode-mismatched configurations are also implemented in dual-beam technique. In the first case, beam waists of both beams are made to coincide inside the sample. In the latter, the sample is placed in the beam waist of pump beam and the beam waists of the pump and probe beams are spatially separated.

In our thermal lens experimental setup as shown in Fig. 3, sample was pumped using a DPSS CW laser operating at 403 nm with maximum power 100mW. The detection of thermal lens signal was achieved by making use of a 4 mW CW He–Ne laser at 632.8 nm wavelength. Both pump and probe beams were aligned in a collinear mode-matched configuration. In collinear configuration, pump and probe beam propagate coaxially in the sample, which creates longer interaction length of the two beams providing a good sensitivity.

A mechanical chopper was used to modulate the pump beam intensity. By adjusting the chopping frequency and sample position, maximum intensity TL signal can be obtained. The chopping frequency is fixed at 3 Hz for all measurements. As the nonmodulated probe beam passes through the irradiated region, a diverging lens effect and thermal blooming occurs [15, 49, 51]. The change in probe beam intensity is measured using a photodetector–DSO system. Time-dependent probe-beam intensity is found to follow the expression [52]:

$$I(t) = I(0)\left[1 - \frac{\theta}{1+\frac{t_c}{2(t-t_0)}} + \frac{\theta^2}{2\left(1+\frac{t_c}{2(t-t_0)}\right)^2}\right]^{-1}. \quad (1)$$

The probe beam phase shift θ is related to thermal power radiation:

$$\theta = \frac{P_{th}\left(\frac{dn}{dT}\right)}{\lambda_L k}, \quad (2)$$

where λ_L is the excitation laser wavelength. Characteristic time for thermal diffusivity t_c is given by

$$t_c = \omega^2\left(\frac{\rho C_p}{4k}\right). \quad (3)$$

The thermal diffusivity α is given by

$$\alpha = \frac{k}{\rho C_p}. \quad (4)$$

Using Eq. (4), Eq. (3) becomes

$$t_c = \frac{\omega^2}{4\alpha}. \quad (5)$$

The parameters θ and t_c can be estimated by curve fitting the experimental data to time-dependent intensity (Eq. 1).

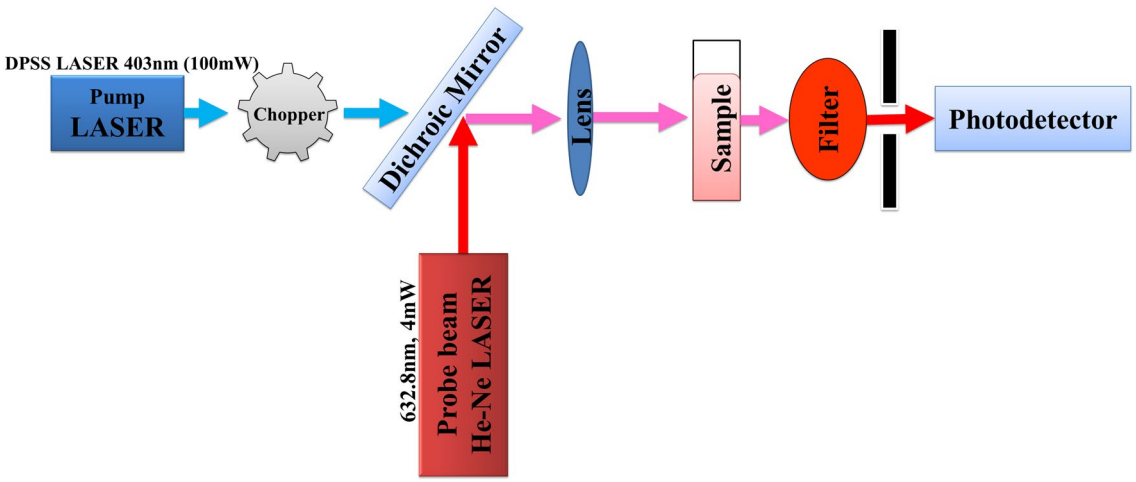

Fig. 3 Dual-beam collinear thermal lens experimental set up

The uncertainty in the determination of beam radius can lead to error in the TL technique. To eliminate this uncertainty, experimental setup has been calibrated by measuring the thermal diffusivity of deionised water as reported in the literature [15]. The measured TL signal is shown in Fig. 4, where the calculated value of diffusivity is 1.41×10^{-7} m^2/s as compared to the diffusivity value of water 1.43×10^{-7} m^2/s. The estimated and theoretical values are thus found to be comparable and all further measurements were made under same experimental conditions. Thermal diffusivity of the unknown sample can be determined by the following equation:

$$\alpha_{\text{sample}} = \alpha_{\text{water}} \frac{t_c^{\text{water}}}{t_c^{\text{sample}}}. \quad (6)$$

3 Results and discussion

To understand particle size and concentration dependence on thermal diffusivity, ZnO nanoparticles with different sizes were dispersed in water for concentrations ranging from 0.02 to 0.1 mg/ml. The thermal diffusivity of these ZnO nanocolloids was measured by fitting theoretical TL signal (Eq. 1) to the experimentally recorded signal. The resulting thermal diffusivity values are summarized in Table 1. It is clear that both particle size and concentration are effectively influencing the thermal diffusivity. All the measurements are triplicated and the uncertainty was found to be in the order of 10^{-4}.

3.1 Nanoparticle size

Figure 5 shows the variation of thermal diffusivity value of water-based ZnO nanofluid as a function of particle size at constant concentration. From the obtained results, it is clear that thermal diffusivity increases with the size of nanoparticles. While the thermal diffusivity increases slightly for samples A, B and C, there is a considerable increase in the diffusivity for sample D compared to other samples at all concentrations. This result indicates that there is an optimum particle size for the enhancement of thermal properties.

Phonon scattering effect and interfacial thermal contact are the main reasons for the enhancement in thermal diffusivity with particle size. When the particle size reaches

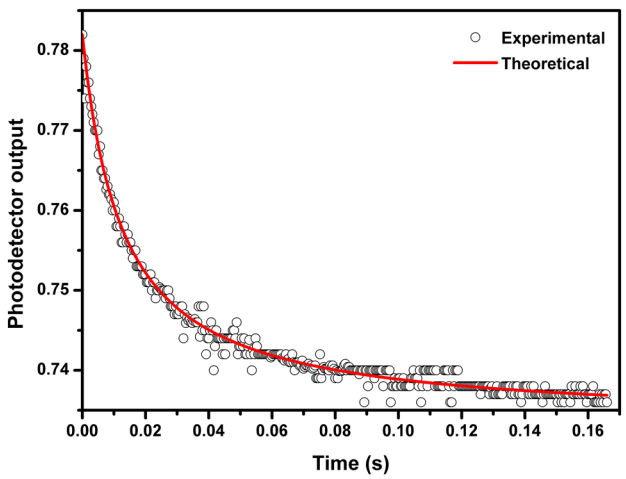

Fig. 4 Typical thermal lens signal recorded for water

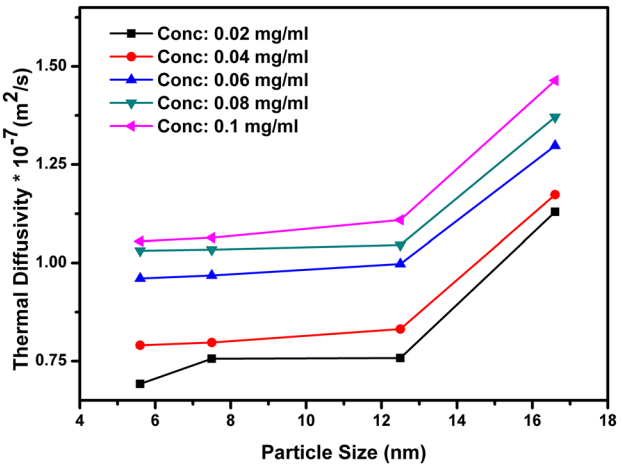

Fig. 5 Thermal diffusivity of ZnO nanofluid with varying particle size

Table 1 Thermal diffusivity of ZnO nanofluid for different particle size and concentration

Con (mg/ml)	Size 5.6 ± 0.61 nm		Size 7.5 ± 1.7 nm		Size 12.5 ± 1.4 nm		Size 16.6 ± 2.2 nm	
	t_c (s)	$\alpha\times10^{-7}$ (m^2/s)	t_c (s)	$\alpha\times10^{-7}$ (m^2/s)	t_c (s)	$\alpha\times10^{-7}$ (m^2/s)	t_c (s)	$\alpha\times10^{-7}$ (m^2/s)
0.02	0.0529	0.6919	0.0484	0.7562	0.0483	0.7578	0.0324	1.1296
0.04	0.0463	0.7905	0.0459	0.7974	0.0440	0.8318	0.0312	1.1731
0.06	0.0381	0.9606	0.0378	0.9683	0.0367	0.9977	0.0282	1.2979
0.08	0.0355	1.0311	0.0354	1.0339	0.0350	1.0457	0.0267	1.3708
0.1	0.0347	1.0548	0.0344	1.0640	0.0330	1.1091	0.0250	1.4640

the order of phonon mean free path, the phonon scattering effect is reduced [49, 50, 53, 54]. This increases the thermal diffusivity value. The interfacial thermal contact resistance between water and solid surfaces affects the thermal transporting behaviour of the fluid. Interfacial thermal resistance/Kapitza resistance is dominant for smaller particle sizes. The poor contact between small size nanoparticles and surrounding liquid decreases the thermal conductivity [54, 55].

3.2 Concentration

From the concentration dependence of thermal diffusivity, shown in Fig. 6, it is clear that a rise in the nanoparticle concentration increases thermal diffusivity. Sample D shows the largest variation in thermal diffusivity compared to the other samples. It can also be noticed that at particular concentration (0.1 mg/ml), the thermal diffusivity of ZnO nanofluid is higher than that of the base fluid (water).

According to the dynamical models, increase in thermal conductivity depends on various parameters such as Brownian motion assisted micro-convection, convective heat transfer, lowering of heating resistance, nanoparticle size and shape [49, 53, 56, 57]. Since the specific heat capacity of solids is lower than that of fluids, the nanofluid possesses lower specific heat capacity than that of the base fluid, as predicted by thermal equilibrium model [58]. Specific heat capacity also decreases with increase in the nanoparticle concentration. Increase in thermal conductivity and decrease in specific heat capacity are contributing to the observed enhancement of the thermal diffusivity [49]. Also, the increase in optical absorption with nanoparticle concentration leads to an enhancement in thermal diffusivity [53, 55] .

Figure 7 depicts the variation of thermal diffusivity with the concentration of nanoparticles indicating the role of nanoparticle concentration in the stability of nanofluid. For a particular concentration, the diffusivity of nanofluid is higher than that of the base fluid. Above this concentration, diffusivity tends to decrease. The stability of the dispersion is a primary prerequisite for the thermal nanofluid [6, 13, 59]. Stability of the ZnO nanofluid was determined by measuring the zeta potential (Horiba SZ-100). Table 2 depicts the zeta potential values of ZnO nanoparticle of size 16.6 nm at different concentrations. If the zeta potential value is greater than ±60 mV, the nanofluid is said to have excellent stability. Nanofluid with zeta potential value near ±45 mV is stable and that with value near to ±30 mV is moderately stable [18, 33, 60]. From Table 2, we understand that 0.1 mg/ml is optimum concentration, in which nanofluid possesses good stability.

When the concentration is increased beyond the maximum limit, the stability of the dispersion gets distorted and there is a tendency for the formation of aggregates. The aggregated nanoparticles get precipitated out of the fluids and settle down, which cause the reduction in original

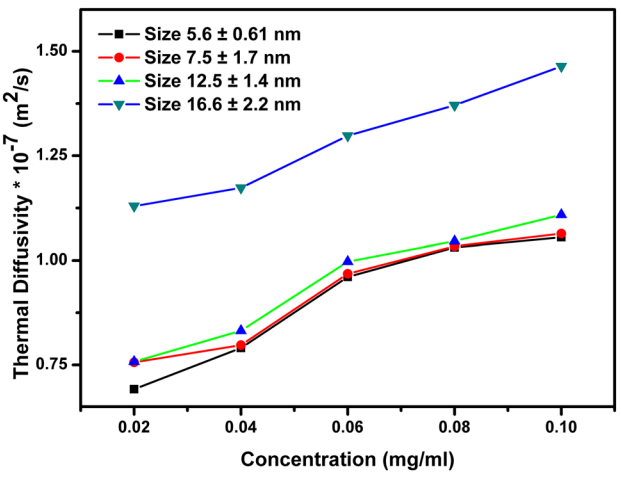

Fig. 6 Thermal diffusivity of ZnO nanofluid with varying concentration

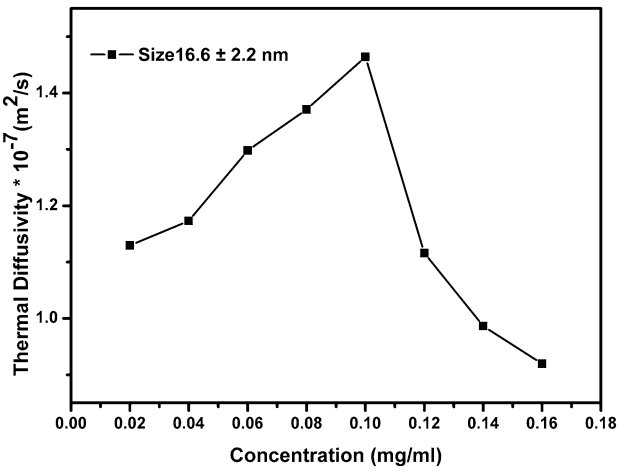

Fig. 7 Thermal diffusivity of ZnO nanofluid with varying concentration of sample D

Table 2 Concentration-dependent zeta potential of sample D

Concentration (mg/ml)	Zeta potential (mV)
0.02	−30.6
0.04	−31.2
0.06	−32.8
0.08	−33.5
0.1	−45.3
0.12	−28
0.14	−27.2
0.16	−26.4

properties (heat transfer enhancement) of the nanofluid. The dispersion behaviour of nanofluids depends on various microscopic forces such as gravitational force, Brownian force, viscous force and inter-particle interaction force [13, 59, 61]. Inter particle interaction force plays a dominant role in the dispersion behaviour of nanofluids compared to other forces. During the interaction, the attractive van der Waals force tends to aggregate the neighbouring nanoparticles. Inter-particle distance and shape of nanoparticles affects the aggregation rate. At short distances, the attractive force (van der Waals force) dominates over the repulsive force (electrostatic force). To overcome the attractive interaction, mainly two types of the dispersion mechanisms are developed to increase the repulsive inter particle interaction, namely electrostatic stabilization and steric stabilization. In electrostatic stabilization, surface charges are introduced into the colloidal solution, and an equal number of counter ions will surround the charged nanoparticles to maintain over all charge neutrality. In steric stabilization, macromolecules (long chain polymers) are attached on the surface of the nanoparticles which screen the van der Waals interaction. So the dispersion stability of nanofluid is further improved by surface modifications [5, 6, 61].

Thermal conductivity (k) of sample D (0.1 mg/ml) was calculated using Eq. (4). From the literature [62], fluid density (ρ) is 0.995 g/cm^3 and the specific heat capacity is $C_p = 4.185$ J/g K. So the thermal conductivity (k) was found to be 0.6108 W/mK. The thermal conductivity of copper nanoparticles as reported by John et al. is 0.512 W/mK [62]. The present study suggests that ZnO nanoparticles can be used in potential cooling applications.

We have estimated the thermal diffusivity of water-based ZnO nanoparticles without any surface treatments. Results show that at a particular size and concentration of nanoparticles, the fluid shows an enhancement in thermal diffusivity than that of the base fluid. According to the literature, the morphological aspects and the surfactant treatments can further improve the thermal properties. Works along these lines are under progress in our laboratory.

4 Conclusion

The present study investigates the effect of particle size and concentration on the thermal diffusivity of the water-based ZnO nanofluid. Thermal diffusivity is found to increase with the particle size and the concentration. This increment is due to the phonon scattering at the interface of liquid, Kapitza resistance and optical absorption. The noticeable result is that the enhanced thermal diffusivity is observable at an optimum value of concentration and particle size. This work suggests that by optimizing the dependent factors, the water-based ZnO nanofluids can be used as coolant for thermoelectric devices.

Acknowledgements Authors acknowledge Science and Engineering Research Board (SERB) Grant no. EEQ/2018/000468, Cochin University of Science and Technology, for the financial assistance.

References

1. A. Gupta, R. Kumar, Role of Brownian motion on the thermal conductivity enhancement of nanofluids. Appl. Phys. Lett. **223102**, 2010–2013 (2011). https://doi.org/10.1063/1.2816903
2. S.M.S. Murshed, C.A.N. De Castro, Superior thermal features of carbon nanotubes-based nano fluids—a review. Renew. Sustain. Energy Rev. **37**, 155–167 (2014). https://doi.org/10.1016/j.rser.2014.05.017
3. E.M. Languri, J. Davidson, K. Nawaz, W. Johnson, F. Mashali, D. Kerns, G. Cunningham, Thermo-physical properties of diamond nanofluids: a review. Int. J. Heat Mass Transf. **129**, 1123–1135 (2018). https://doi.org/10.1016/j.ijheatmasstransfer.2018.10.033
4. E.M. Cárdenas Contreras, G.A. Oliveira, E.P. Bandarra Filho, Experimental analysis of the thermohydraulic performance of graphene and silver nanofluids in automotive cooling systems. Int. J. Heat Mass Transf. **132**, 375–387 (2019). https://doi.org/10.1016/j.ijheatmasstransfer.2018.12.014
5. R. Saidur, K.Y. Leong, H.A. Mohammad, A review on applications and challenges of nanofluids. Renew. Sustain. Energy Rev. **15**, 1646–1668 (2011). https://doi.org/10.1016/j.rser.2010.11.035
6. J. Sarkar, A critical review on convective heat transfer correlations of nanofluids. Renew. Sustain. Energy Rev. **15**, 3271–3277 (2011). https://doi.org/10.1016/j.rser.2011.04.025
7. V. Trisaksri, S. Wongwises, Critical review of heat transfer characteristics of nanofluids. Renew. Sustain. Energy Rev. **11**, 512–523 (2007). https://doi.org/10.1016/j.rser.2005.01.010
8. W.H. Azmi, K.V. Sharma, R. Mamat, G. Naja, M.S. Mohamad, The enhancement of effective thermal conductivity and effective dynamic viscosity of nano fluids—a review. Renew. Sustain. Energy Rev. **53**, 1046–1058 (2016). https://doi.org/10.1016/j.rser.2015.09.081
9. S. Krishnamurthy, P. Bhattacharya, P.E. Phelan, Enhanced mass transport in nanofluids. Nano Lett. **6**, 419–423 (2006). https://doi.org/10.1021/nl0522532
10. D. Cabaleiro, L. Colla, F. Agresti, L. Lugo, L. Fedele, Transport properties and heat transfer coefficients of ZnO/(ethylene glycol + water) nanofluids. Int. J. Heat Mass Transf. **89**, 433–443 (2015). https://doi.org/10.1016/j.ijheatmasstransfer.2015.05.067
11. M. Kahani, R.G. Jackson, G. Rosengarten, Experimental investigation of TiO_2/water nano fluid droplet impingement on nanostructured surfaces. IEC Res. (2016). https://doi.org/10.1021/acs.iecr.5b04465
12. A. Ijam, R. Saidur, P. Ganesan, A. Moradi Golsheikh, Stability, thermo-physical properties, and electrical conductivity of graphene oxide-deionized water/ethylene glycol based nanofluid. Int. J. Heat Mass Transf. **87**, 92–103 (2015). https://doi.org/10.1016/j.ijheatmasstransfer.2015.02.060
13. X. Wang, A.S. Mujumdar, Heat transfer characteristics of nanofluids: a review. Int. J. Therm. Sci. **46**, 1–19 (2007). https://doi.org/10.1016/j.ijthermalsci.2006.06.010
14. S. Simpson, A. Schelfhout, C. Golden, S. Vafaei, Nanofluid thermal conductivity and effective parameters. Appl. Sci. (2018). https://doi.org/10.3390/app9010087
15. M. Hari, S. Ani, S. Mathew, B. Nithyaja, V.P.N. Nampoori, P. Radhakrishnan, Thermal diffusivity of nano fluids composed of

rod-shaped silver nanoparticles. Int. J. Therm. Sci. **64**, 188–194 (2013). https://doi.org/10.1016/j.ijthermalsci.2012.08.011
16. L. Yang, K. Du, A comprehensive review on heat transfer characteristics of TiO_2 nanofluids. Int. J. Heat Mass Transf. **108**, 11–31 (2017). https://doi.org/10.1016/j.ijheatmasstransfer.2016.11.086
17. P. Taylor, W. Yu, D.M. France, J.L. Routbort, S.U.S. Choi, Review and comparison of nanofluid thermal conductivity and heat transfer enhancements. Heat Transf. Eng. (2008). https://doi.org/10.1080/01457630701850851
18. W. Yu, H. Xie, A review on nanofluids: preparation, stability mechanisms, and applications. J. Nanomater. (2012). https://doi.org/10.1155/2012/435873
19. S. Mukherjee, P.C. Mishra, P. Caudhuri, Stability of heat transfer nanofluids—a review. ChemBioEng. (2018). https://doi.org/10.1002/cben.201800008
20. E.V. Timofeeva, J.L. Routbort, D. Singh, E.V. Timofeeva, J.L. Routbort, D. Singh, Particle shape effects on thermophysical properties of alumina nanofluids. J. Appl. Phys. (2009). https://doi.org/10.1063/1.3155999
21. M. Hossein, A. Mirlohi, M. Alhuyi, R. Ghasempour, A review of thermal conductivity of various nano fluids. J. Mol. Liq. **265**, 181–188 (2018). https://doi.org/10.1016/j.molliq.2018.05.124
22. N. Sizochenko, M. Syzochenko, A. Gajewicz, J. Leszczynski, T. Puzyn, Predicting physical properties of nano fluids by computational modeling. J. Phys. Chem. C **121**, 1910–1917 (2016). https://doi.org/10.1021/acs.jpcc.6b08850
23. M.I. Pryazhnikov, A.V. Minakov, V.Y. Rudyak, D.V. Guzei, Thermal conductivity measurements of nanofluids. Int. J. Heat Mass Transf. **104**, 1275–1282 (2017). https://doi.org/10.1016/j.ijheatmasstransfer.2016.09.080
24. W. Yu, H. Xie, L. Chen, Y. Li, Investigation of thermal conductivity and viscosity of ethylene glycol based ZnO nanofluid. Thermochim. Acta **491**, 92–96 (2009). https://doi.org/10.1016/j.tca.2009.03.007
25. G. Huminic, A. Huminic, Application of nanofluids in heat exchangers: a review. Renew. Sustain. Energy Rev. **16**, 5625–5638 (2012). https://doi.org/10.1016/j.rser.2012.05.023
26. H.A. Badran, Thermal properties of a new dye compound measured by thermal lens effect and Z-scan technique. Appl. Phys. B. (2015). https://doi.org/10.1007/s00340-015-6068-2
27. H. Li, Y. He, Y. Hu, B. Jiang, Y. Huang, Thermophysical and natural convection characteristics of ethylene glycol and water mixture based ZnO nanofluids. Int. J. Heat Mass Transf. **91**, 385–389 (2015). https://doi.org/10.1016/j.ijheatmasstransfer.2015.07.126
28. V. Mikkola, S. Puupponen, H. Granbohm, K. Saari, A. Seppälä, Influence of particle properties on convective heat transfer of nano fluids. Int. J. Therm. Sci. **124**, 187–195 (2018). https://doi.org/10.1016/j.ijthermalsci.2017.10.015
29. A.A. Nadooshan, An experimental correlation approach for predicting thermal conductivity of water-EG based nanofluids of zinc oxide. Phys. E Low Dimens. Syst. Nanostruct. **87**, 15–19 (2017). https://doi.org/10.1016/j.physe.2016.11.004
30. J.R.V. Peñas, J.M.O. De Zárate, M. Khayet, Measurement of the thermal conductivity of nanofluids by the multicurrent hot-wire method. J. Appl. Phys. **104**, 1–8 (2008). https://doi.org/10.1063/1.2970086
31. C. Kleinstreuer, Y. Feng, Experimental and theoretical studies of nanofluid thermal conductivity enhancement: a review. Nanoscale Res. Lett. **6**, 1–13 (2011)
32. G. Paul, M. Chopkar, I. Manna, P.K. Das, Techniques for measuring the thermal conductivity of nanofluids: a review. Renew. Sustain. Energy Rev. **14**, 1913–1924 (2010). https://doi.org/10.1016/j.rser.2010.03.017
33. R. Choudhary, D. Khurana, A. Kumar, S. Subudhi, Stability analysis of Al_2O_3/water nanofluids. J. Exp. Nanosci. (2017). https://doi.org/10.1080/17458080.2017.1285445
34. M.L.B.J.H. Rohlig, J. Mura, J.R.D. Pereira, A.J. Palangana, A.N. Medina, A.C. Bento, Thermal lens temperature scanning for quantitative measurements in complex fluids. Braz. J. Phys. **32**, 575–583 (2002)
35. A. Marcano, H. Cabrera, M. Guerra, R.A. Cruz, C. Jacinto, T. Catunda, Optimizing and calibrating a mode-mismatched thermal lens experiment for low absorption measurement. J. Opt. Soc. Am. B. **23**, 1408–1413 (2006)
36. L.A. Skvortsov, Laser photothermal spectroscopy of light-induced absorption. Quantum Electron. **43**, 1–13 (2017). https://doi.org/10.1070/QE2013v043n01ABEH014912
37. S. Instruments, N. Gorica, Analytical thermal lens instrumentation. Am. Inst. Phys. **67**, 1–18 (1996). https://doi.org/10.1063/1.1147512
38. J.P. Gordon, R.C.C. Leite, R.S. Moore, S.P.S. Porto, J.R. Whinnery, Long transient effects in lasers with inserted liquid samples. J. Appl. Phys. (1965). https://doi.org/10.1063/1.1713919
39. S.J. Sheldon, L.V. Knight, J.M. Thorne, Laser-induced thermal lens effect: a new theoretical model. Appl. Opt. **21**, 1663–1669 (1982)
40. R.D. Snook, R.D. Lowe, Thermal lens spectrometry. Analyst **120**, 2051–2068 (1995)
41. A. Chemistry, S.N. Bendrysheva, M. Sciences, Advances in thermal lens spectrometry. J. Anal. Chem. (2015). https://doi.org/10.1134/S1061934815030168
42. R. Silva, M.A.C. De Araújo, P. Jali, S.G.C. Moreira, P.A. Jr, C. Paulo, R. Silva, M.A.C. De Ara, P. Jali, G.C. Sanclayton, Thermal lens spectrometry: optimizing amplitude and shortening the transient time. AIP Adv. (2011). https://doi.org/10.1063/1.3609966
43. S. Kumar, H. Lee, T. Yoon, C.N. Murthy, J. Lee, Morphological control over ZnO nanostructures from self-emulsion polymerization. Cryst. Growth Des. **117**, 3905–3911 (2016). https://doi.org/10.1021/acs.cgd.6b00479
44. P. Rai, W. Kwak, Y. Yu, Solvothermal synthesis of ZnO nanostructures and their morphology-dependent gas-sensing properties. Appl. Mater. Interfaces **5**, 3026–3032 (2013). https://doi.org/10.1021/am302811h
45. Y. Zhang, J. Xu, Q. Xiang, H. Li, Q. Pan, P. Xu, Brush-like hierarchical ZnO nanostructures: synthesis, photoluminescence and gas sensor properties. J. Phys. Chem. C **113**, 3430–3435 (2009)
46. M. Raula, H. Rashid, T.K. Paira, E. Dinda, T.K. Mandal, Ascorbate-assisted growth of hierarchical ZnO nanostructures: sphere, spindle, and flower and their catalytic properties. Langmuir **26**, 8769–8782 (2010). https://doi.org/10.1021/la904507q
47. M. Ramya, T.K. Nideep, K.R. Vijesh, V.P.N. Nampoori, M. Kailasnath, Synthesis of stable ZnO nanocolloids with enhanced optical limiting properties via simple solution method. Opt. Mater. (Amst) **81**, 30–36 (2018). https://doi.org/10.1016/j.optmat.2018.05.007
48. M. Andika, G. Chung, K. Chen, S. Vasudevan, Excitation temporal pulse shape and probe beam size effect on pulsed photothermal lens of single particle. Opt. Soc. Am. **27**, 796–805 (2010)
49. J. John, L. Thomas, B.R. Kumar, A. Kurian, Shape dependent heat transport through green synthesized gold nanofluids. J. Phys. D. Appl. Phys. (2015). https://doi.org/10.1088/0022-3727/48/33/335301
50. E. Shahriari, M. Moradi, M. Raeisi, An experimental study of thermal diffusivity of Au nanoparticles: effects of concentration particle size. J. Theor. Appl. Phys. **10**, 259–263 (2016). https://doi.org/10.1007/s40094-016-0224-x
51. S. Ani, M. Hari, S. Mathew, G. Sharma, V.M. Hadiya, P. Radhakrishnan, V.P.N. Nampoori, Thermal diffusivity of rhodamine 6G incorporated in silver nanofluid measured using mode-matched thermal lens technique. Opt. Commun. **283**, 313–317 (2010). https://doi.org/10.1016/j.optcom.2009.10.016

52. J.R. Whinnery, Laser measurement of optical absorption in liquids. Acc. Chem. Res. **7**, 225–231 (1974)
53. R. Herrera-aquino, Green synthesis of silver nanoparticles contained in centrifuged citrus oil and their thermal diffusivity. Int. J. Thermophys. **123**, 1–10 (2019). https://doi.org/10.1007/s10765-018-2466-0
54. E. Shahriari, The effect of nanoparticle size on thermal diffusivity of gold nano-fluid measured using thermal lens technique. JEOS Rapid Publ **13026**, 1–4 (2013)
55. A. Viswanathan, S. Udayan, P.N. Mus, V.P.N. Nampoori, S. Thomas, Enhancement of defect states assisted thermal diffusivity in solution-processed GeSeSb chalcogenide glass matrix on silver incorporation. J. Non Cryst. Solids (2018). https://doi.org/10.1016/j.jnoncrysol.2018.09.039
56. X. Liu, X. Xing, Y. Li, N. Chen, I. Djerdj, Y. Wang, Controllable synthesis and change of emission color from green to orange of ZnO quantum dots using different solvents. New J. Chem. **39**, 2881–2888 (2015). https://doi.org/10.1039/C5NJ00070J
57. G.A. López-muñoz, J.A. Balderas-lópez, J. Ortega-lopez, J.A. Pescador-rojas, J.S. Salazar, Thermal diffusivity measurement for urchin-like gold nanofluids with different solvents, sizes and concentrations/shapes. Nanoscale Res. Lett. **667**, 1–7 (2012)
58. V.M. Lenart, N.G.C. Astrath, R.F. Turchiello, G.F. Goya, Thermal diffusivity of ferrofluids as a function of particle size determined using the mode-mismatched dual-beam thermal lens technique. J. Appl. Phys. **123**, 085107 (2018). https://doi.org/10.1063/1.5017025
59. P.D. Shima, J. Philip, B. Raj, P.D. Shima, J. Philip, B. Raj, Role of microconvection induced by Brownian motion of nanoparticles in the enhanced thermal conductivity of stable nanofluids. Appl. Phys. Lett. **94**, 223101 (2009). https://doi.org/10.1063/1.3147855
60. N. Ali, J.A. Teixeira, A. Addali, A review on nanofluids: fabrication, stability, and thermophysical properties. J. Nanomater. **2018**, 1–33 (2018)
61. F. Yu, Y. Chen, X. Liang, J. Xu, C. Lee, Q. Liang, P. Tao, Progress in natural science: materials international dispersion stability of thermal nano fl uids. Prog. Nat. Sci. Mater. Int. **27**, 531–542 (2017). https://doi.org/10.1016/j.pnsc.2017.08.010
62. J. John, R. Mary, I. Rejeena, R. Jayakrishnan, S. Mathew, V. Thomas, A. Mujeeb, Nonlinear optical limiting and dual beam mode matched thermal lensing of nano fluids containing green synthesized copper nanoparticles. J. Mol. Liq. **279**, 63–66 (2019). https://doi.org/10.1016/j.molliq.2019.01.125